Infrared Spectroscopic Characterization of cPLA$_2$α C2 Domain

A Major Qualifying Project Report

(Chemistry)

submitted to the Faculty of

WORCETER POLYTECHNIC INSTITUTE

in partial fulfillment of the requirements for the

Bachelor of Science Degree

Yunqiu Sun

04/25/2014

Advisor: Dr. Arne Gericke

Abstract

Group IV cytosolic phospholipase $A_2\alpha$ ($cPLA_2\alpha$) hydrolyzes membrane phospholipids to produce arachidonic acid and lysolipid. The C2 domain of the enzyme is involved in the Ca^{2+} -dependent translocation of the enzyme to the membrane and has a structure of 8 anti-parallel β sheets composed of 132 amino acids. Ceramide-1-phosphate (C1P) enhances the association of the $cPLA_2\alpha$'s C2 domain with membranes. This research project aims to understand the binding properties and secondary structural changes of the $cPLA_2\alpha$ C2 domain in the presence of phosphatidylcholine (PC). We optimized the protein expression conditions to obtain the $cPLA_2\alpha$ C2 domain un-aggregated and in sufficient quantity. Initial FTIR-ATR experiments confirmed the β-sheet structure of the protein alone and in the presence of PC.

Acknowledgements

I would like to first express my great appreciation for my advisor Dr. Arne Gericke, for being a great advisor that provides instructive comments and timely feedback, and for being a humorous advisor that cheered me up through my first scientific research project.

Second, I would like to appreciate everyone in Arne's lab that supported me through this progress: Rakesh, a great molecular biology instructor, a very patient senior that helped me learned so much about protein purification and expression, and for all the late afternoons that you spent with me to help me get the experiments done on time; Anne-Marie, for that conversation about lab notebook, your P-rex dance that kept my heads up for my research, and your ride through the snow days; Katie, for teaching me about research since my sophomore year and always been a great friend; Brittany, for your great talk about future directions; and Ann Mondor, for all your hugs and chocolate and cookie treats. I truly regard everyone as a role model of mine for being working hard, willing to learn, and being optimistic about life. The friendship and laughter supported me through my college career.

I also want to thank Professor Robert Dempski for providing me a space in his lab, Sagar Antala and Elizabeth Bafaro for listening to my problems and providing helpful suggestions.

I deeply appreciate WPI, which provided this great opportunity, and to everyone else that helped me in this project.

Table of Contents

Introduction

Functional Role of C2 Domain

Group IVA cytosolic phospholipase A_2 (cPLA$_2\alpha$) is an enzyme that liberates arachidonic acid (AA) from the sn-2 position of membrane phospholipids in response to inflammatory agonist [1-3]. The protein exhibits two major domains: an N-terminal lipid binding C2 domain and a catalytic domain. The C2 domain binds to zwitterionic lipids and docks to phosphatidylcholine (PC)-rich internal membranes in mammalian cells in a Ca^{2+} dependent manner [4]. The endoplasmic reticulum (ER) and the Golgi have been suggested as targets for cPLA$_2\alpha$ translocation, while cPLA$_2\alpha$ plasma membrane association has not been observed [5]. Following the membrane binding and penetration of the C2 domain, the catalytic domain releases AA from zwitterionic lipids. The generation of AA initiates pathways, such as the 5-lipoxygenase and the cyclooxygenase (COX) pathway, leading to eicosanoid synthesis, which has been implicated in heart disease [6], asthma [7], arthritis [8], cancers [9], and Alzheimer's disease [10].

The C2 domain used for this study is tagged with 6 Histidines on the C terminal end is composed of 132 residues, and its molecular weight is about 15kDa (see Figure 1 for the amino acid sequence). The secondary structure is dominated by a beta-sandwich composed of 8 β-strands that coordinates two or three calcium ions (Figure 2). The coordination sites are located at one end of the β-sandwich.

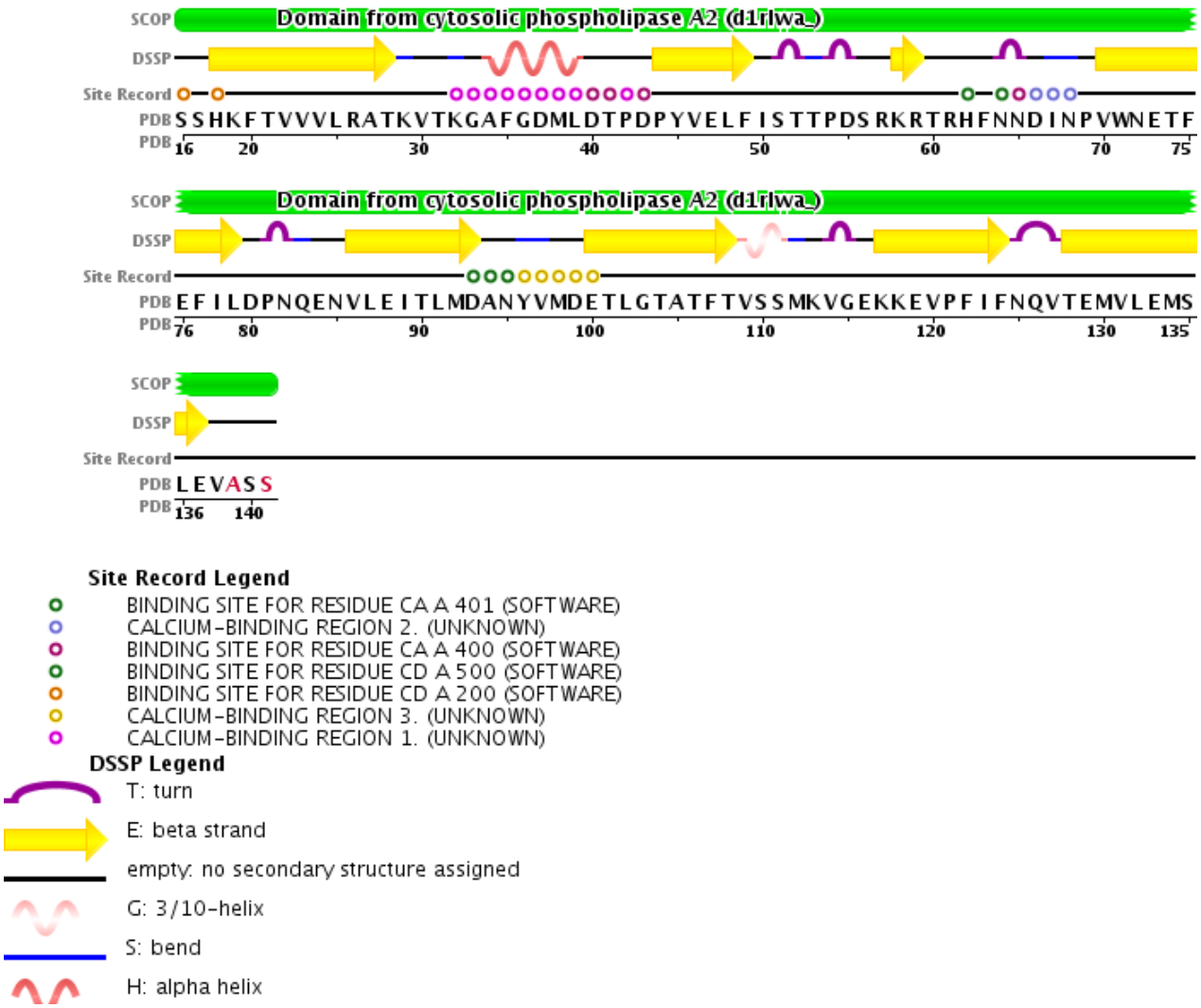

Figure 1. The amino acid sequence of cPLA$_2\alpha$ C2 domain

Figure 2. 3D view of the secondary structure of cPLA$_2$α C2 domain

Lipid Binding of cPLA$_2$α C2 Domain

As previously mentioned, the C2 domain is an N-terminal lipid-binding domain. Most C2 domains bind to membranes in a Ca^{2+} dependent manner via the three calcium-binding regions (CBRs) that are located at one end of the β sandwich. Modulating the presence or absence of different types of phospholipids can help determine the different Ca^{2+} binding affinities [4]. The previous studies characterized the binding between the C2 domain and PC and phosphatidylinositol 4,5-bisphosphate (PI(4,5)P_2). The current research has focused on the binding between the C2 domain and Ceramide-1-Phosphate (C1P). C1P is a potent bioactive lipid, which has a substantial affinity for the cationic patch in the β-groove of the C2 domain.

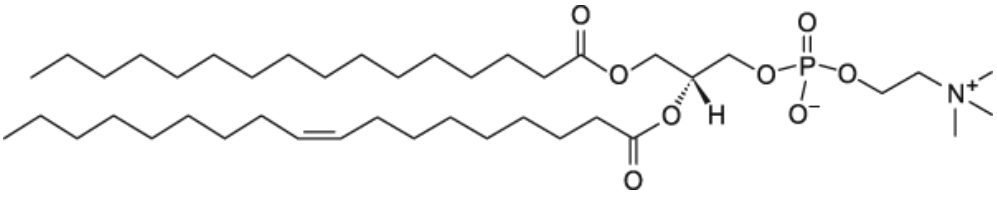

Figure 3. The structure of 1-palmitoyl-2-oleoyl-*sn*-glycero-3-phosphocholine (POPC)

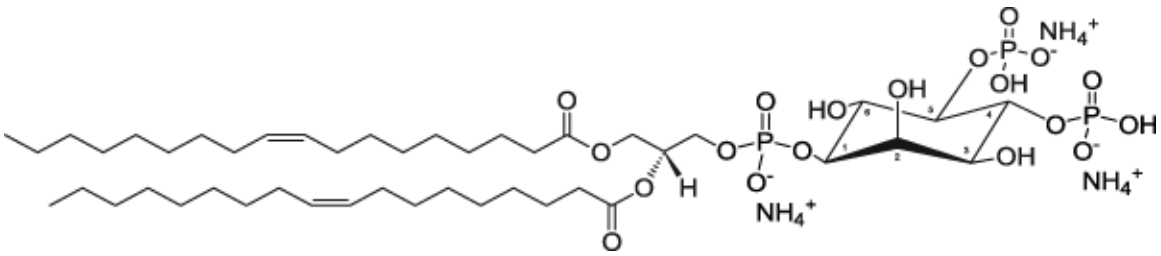

Figure 4. The structure of 1,2-dioleoyl-*sn*-glycero-3-phospho-(1'-myo-inositol-4',5'-bisphosphate) (18:1 PI(4,5)P_2)

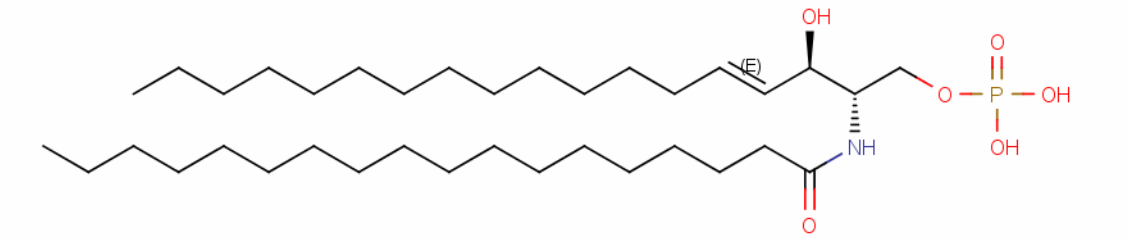

Figure 5. The structure of D-erythro-Ceramide C18 1 Phosphate used to study the C1P binding site in the C2 domain

cPLA$_2$α C2 Domain C1P Binding Specificity

C1P is of specific interest because it is the only membrane-embedded anionic lipid that has been shown to increase membrane affinity of the cPLA$_2$α C2 domain [11]. As mentioned before, cPLA$_2$α binds to PC membranes in a Ca^{2+} dependent manner. Based on the well-established understanding of the preferential binding of the cPLA$_2$α C2 domain to zwitterionic lipids, C1P containing vesicles show increased binding affinity over PC membranes. The wild type cPLA$_2$α C2 domain bound to 3 mol% C1P vesicles ten times stronger than to POPC (1-palmitoyl-2-oleoyl-*sn*-glycero-3-phosphocholine) vesicles alone [4]. The binding of POPC and C1P has been extensively studied, and the binding orientation was validated by site-directed spin labeling and X-ray reflectivity

studies [12,13]. $PI(4,5)P_2$ is also found to increase $cPLA_2\alpha$ affinity for the membrane and enhance $cPLA_2\alpha$ activity, but it binds to $cPLA_2\alpha$ at the catalytic domain while the C1P binds to $cPLA_2\alpha$ at the C2 domain [14].

In previous studies, C1P was shown to regulate the translocation of $cPLA_2\alpha$ and increase the protein's biological activity; however only C1P with an acyl-chain of ≥ 6 carbons, such as C_6-C1P, C_{16}-C1P, $C_{18:1}$-C1P, can efficiently activate $cPLA_2\alpha$ *in vitro*. C1P with acyl-chain<6, such as C_2-C1P, when it binds to the C2 domain, the complex is ineffective in the induction of AA release [15]. Surface Plasmon Resonance (SPR) analysis with different $cPLA_2\alpha$ C2 domain mutants performed by Stahelin et al. identified the C1P binding site in the C2 domain [4]. Their research showed specific binding of C1P to the cationic β groove ($Arg^{57}/Lys^{58}/Arg^{59}$), which enhances $cPLA_2\alpha$ activity by lowering its membrane dissociation rate. This binding site is the shortest β groove, adjacent to one of the membrane-penetrating CBRs (His^{62} to Asn^{64}), but the binding mechanism is different from the membrane penetration [4] (Figure 6). The SPR data also suggest that the $cPLA_2\alpha$ C2 domain C1P binding specificity is determined by Arg^{59}, Arg^{61}, and His^{62}, and that these amino acids are important for cellular translocation of $cPLA_2\alpha$ [16].

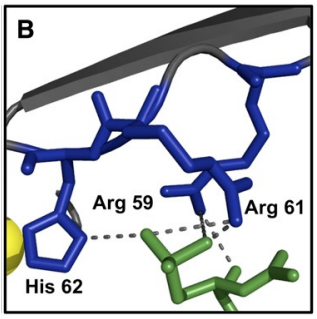

Figure 6. Higher magnification shows more clearly the specific interactions between Arg^{59}, Arg^{61}, and His^{62} and C1P in the C2 domain of $cPLA_2\alpha$.

The most recent studies showed that membrane penetration is a prerequisite for the β groove to make contact with the C1P headgroup. Peripheral proteins, such as those with C2 domains, must penetrate deeply into the membrane to bind to C1P; however, research has not shown any evidence that C1P induces the C2 domain to penetrate deeper into the membrane [17]. Previous research revealed that the C2 domain maximizes its hydrophobic contacts when bound to C1P, rather than increase or induce membrane penetration. Even though the latter is possible, its effect on binding is almost negligible [4]. C1P binding is also expected to contribute to the C2 domain translocation of the catalytic domain to internal membranes even if the C2 domain does not penetrate into membranes.

cPLA$_2$α C2 Domain C1P Binding Orientation under Physiological pH

Molecular Dynamics (MD) simulations have been performed to understand the C1P triggered structural change of the cPLA$_2$α C2 domain upon binding by comparing the C2 domain PC binding in the absence and presence of C1P. When only POPC and Ca^{2+} are present, the domain forms a stable complex with the bilayer, with only a small deviation from the binding orientation. The domain shows even less deviation when C1P is introduced into the bilayer in the presence of Ca^{2+}, which suggests that the domain forms a more stable protein-membrane complex [17]. In addition, C1P further strengthens the binding of the C2 domain in the absence of one Ca^{2+} ion, demonstrating its role in promoting the C2 domain docking to zwitterionic membranes.

Recently, electron paramagnetic resonance [12] and X-ray reflectivity studies [13] have elucidated the cPLA$_2$α C2 domain orientation in the presence of POPC lipids; however, the orientation of the domain in the presence of C1P is still unknown. MD simulation

suggest that starting with the same orientation as that with only POPC, the domain tilts by ~10° toward the bilayer over the course of the simulation in the presence of C1P [12] (Figure 7). This tilting facilitates formation of stable H bonds between cationic residues and the C1P head group. Compared to PC, C1P's smaller and more deeply buried headgroup at physiological pH supports the 10° tilting as the C1P acyl chains have been found to tilt away from the surface normal in monolayer experiments [18]. Thus, Arg^{59}, Arg^{61}, and His^{62} residues may further facilitate formation of hydrogen bonds by extending their side chains toward the bilayer. Current research is focused on the C2 domain binding mechanism and how it recognizes C1P over phosphatidic acid (PA), which has the same headgroup.

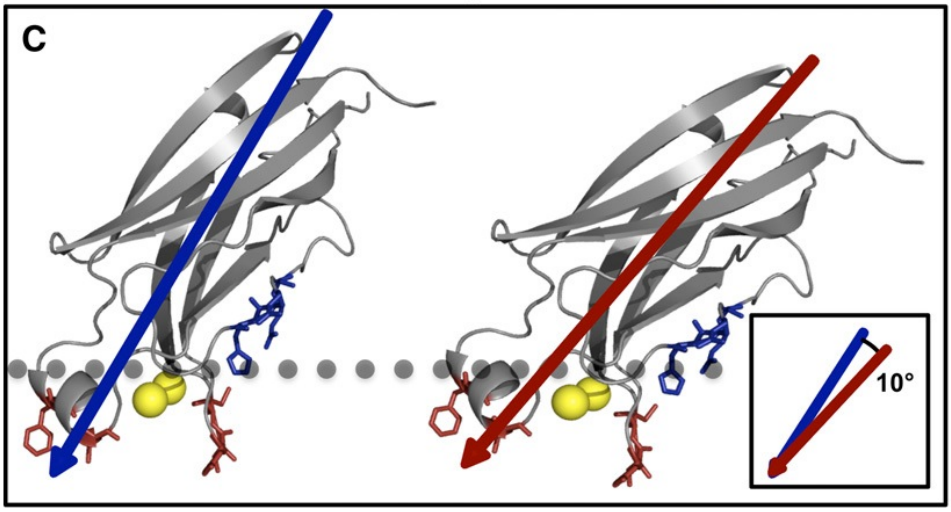

Figure 7. The C2 domain rotates upon membrane docking to bind C1P embedded in the membrane.

pH dependent cPLA$_2$α C2 domain Binding Orientation in the Presence of Ceramide-1-Phosphate

Binding studies show that cPLA$_2$α C2 domain C1P interaction is pH dependent. This pH dependent interaction highlights the importance of the His^{62} protonation for the

proper coordination of the C1P headgroup. The high affinity of C1P to the C2 domain in an acidic environment has potentially important physiological implications, because the intracellular pH can vary during inflammation [19] or cancer [20] with a more profound acid pH. Because $cPLA_2\alpha$ has been implicated in inflammatory diseases and cancers, the pH dependence of $cPLA_2\alpha$ translocation and activation at acidic pH warrants further investigation.

Objectives of This Research

The $cPLA_2\alpha$ C2 domain orientation in the presence of both POPC lipids and C1P is still unknown though MD simulation results suggest structural and orientational changes. This project aims to characterize the change of the secondary structure and orientation (tilting angle) when C1P binds to $cPLA_2\alpha$ C2 domain *in vitro* using Fourier transformation infrared attenuated total reflection (FTIR-ATR) spectroscopy. To achieve this goal, the expression and purification of $cPLA_2\alpha$ C2 domain was first optimized to obtain sufficient quantities of protein for the biophysical studies. The FTIR-ATR technique was used to monitor the changes in the secondary structure of $cPLA_2\alpha$ C2 domain upon lipid binding. The secondary structure of the $cPLA_2\alpha$ C2 domain was studied in the absence and presence of POPC, to understand how lipid binding affects the secondary structure of the C2 domain.

Materials and Methods

Materials

The DNA stock of cPLA2α C2 domain with a C-terminal 6HIS tag was received from Dr. Robert Stahelin's group at University of Notre Dame and stored at -20°C. POPC was purchased from Avanti Polar Lipids (Alabaster, AL). All the other chemicals used in this study are listed alphabetically in Appendix A. All the acronyms are listed in Appendix B. All the buffers used in the protein expression and purification are listed in Appendix C.

Bacterial Expression and Purification of cPLA$_2$α C2 Domain

Transformation of cPLA$_2$α C2 domain in NiCo21 (DE3) *E.coli* strain

The cPLA$_2$α C2 domain was transformed into NiCo21(DE3) *E. coli* strain (New England BioLabs). One microliter of DNA stock was added to the NiCo21(DE3) cells and kept on ice for 30 min followed by incubating at 42°C for 45 s to give a heat shock and then placed on ice for 2 min. Next, 500µL of SOC media was added and the cells were incubated in a shaker at 37°C for 1 hr. After the cells were recovered, 50µL of the transformation mix was added and spread evenly onto a kanamycin (30µg/mL) LB agar plate. The agar plate was incubated at 37°C overnight. One bacterial colony was inoculated into 30mL of LB broth with 30µg/mL kanamycin and incubated at 37°C overnight at 180rpm. The next day, the glycerol stocks of NiCo21 (DE3) harboring cPLA$_2$α C2 domain culture containing 20 percent of autoclaved glycerol were prepared and aliquots of 1mL were stored at -80°C.

Expression of the cPLA$_2$α C2 domain

A starter culture (6mL LB broth) supplemented with 30µg/mL kanamycin was inoculated from the previously prepared glycerol stocks and incubated in a shaker at 37°C overnight. The overnight culture was added into one liter of autoclaved 2X YT broth containing 30µg/mL kanamycin along with 200µL of KFO80 anti-foaming reagent. The culture was grown at 37°C to an OD_{600nm} of 0.6-0.8. The culture was shifted to 18 °C, and after 30 min protein expression was induced with 0.1mM IPTG. After overnight induction, the cells were harvested by centrifugation at 5,000rpm for 10min at 4 °C with Beckman Coulter JA-25.5 Rotor. 100mL of phosphate buffered saline (PBS) buffer was mixed with the cells and centrifuged at 5,000rpm for 10min for a wash. Then aliquots of 5g of cell pellet were stored at -20°C for protein purification.

Protein Purification of cPLA$_2$α C2 domain

For protein purification, cells were re-suspended in 30mL of lysis buffer (50mM Tris-HCl, 50mM NaCl, 2mM EDTA, 1mM PMSF, 0.4% (v/v) Triton-X 100, 0.4% (w/v) sodium deoxycholate, pH 8.0**)**. The cells were lysed by sonication for 30 seconds and then placed on ice for 3 min (this was repeated 8 times) (Fisher Scientific, Sonic Dismembrator Model 100, Fair Lawn, NJ). After sonication, the cell lysate was centrifuged at 13,200 rpm for 20 min at 4°C. The pellet containing the inclusion bodies was re-suspended into 30mL of wash buffer #1 (50mM Tris-HCl, 50mM NaCl, 2mM EDTA, 0.8% (v/v) Triton-X, 0.8% (w/v) sodium deoxycholate, pH 8.0) and briefly sonicated followed by centrifugation at 13,200 rpm for 20 min at 4°C. The pellet was given a second wash with 30mL of wash buffer #2 (50mM Tris-HCl, 5M Urea, 5mM

EDTA, pH 8.0). Again, the re-suspension was briefly sonicated and centrifuged at 13,200rpm for 20 min at 4°C. The washed inclusion bodies were solubilized with 30mL of solubilizing buffer (50mM Tris-HCl, 8M Urea, 5mM EDTA, pH 8.0) and incubated on a rocker for 60 min at room temperature. The insoluble matter was removed by centrifugation at 13,200 rpm for 30 min at 4°C. The supernatant was dialyzed against 2 L of dialysis buffer #1 (50mM Tris-HCl, 1.5M Urea, pH 8.0) overnight and then was dialyzed 2 times against 1L of dialysis buffer #2 (50mM Tris-HCl, pH 8.0) for 8hr at 4°C.

The refolded C2 domain was purified using a HisPur Ni-NTA agarose column (Thermo Scientific, Pittsburg, PA). The column was equilibrated with 25mL of binding buffer (50mM Tris-HCl, 150mM NaCl**,** 10mM imidazole, pH 8.0). The supernatant was incubated on a rocker for 60 min at 4 °C and then washed with 15mL of binding buffer and 25mL of wash buffer #3 (50mM Tris-HCl, 150mM NaCl, 20mM imidazole, pH 8.0). The protein was eluted with 10mL of elution buffer #1 (20mM HEPES, 150mM NaCl, 400mM imidazole, pH 8.0). Small aliquots from the flow through, wash #1, wash #2 steps from the Ni-NTA agarose column, as well as the protein elution #1 were stored at 4°C for further analysis. The protein was dialyzed against 2L of dialysis buffer #3 (20mM HEPES, 100mM NaCl, pH 7.4) overnight. The C2 domain was then further purified using a Mono Q anion exchange column (Bio-Rad, Hercules, CA). Before loading the protein sample, the column was equilibrated with 5mL of low salt buffer (20mM HEPES, 50mM NaCl, pH 7.4), 10mL of high salt buffer (20mM HEPES, 1M NaCl, pH 7.4), and then again with 15mL of low salt buffer. After the protein was bound to the column, it was washed with 5mL of low salt buffer and eluted with six fractions of 2mL of elution buffer #2 (20mM HEPES, 300mM NaCl, pH 7.4) and 1mL of high salt

buffer. Aliquots of the load and flow through from the Mono Q anion exchange column and all elution fractions were stored at 4°C for further analysis.

Dynamic Light Scattering

The purified protein was analyzed with Dynamic Light Scattering (DLS) to check the size of the protein and to verify that the protein was not aggregated (Malvern, Nano ZS, Worcestershire, UK). 60 µL of the purified protein was added into the quartz batch cuvette and both volume particle size distribution (PSD) and intensity PSD were recorded at room temperature.

SDS-PAGE

The protein samples were characterized by sodium dodecyl sulfate polyacrylamide gel electrophoresis (SDS-PAGE) to check for purity and yield. Spectra Multicolor Broad Range Protein Ladder was used as marker to locate the protein (Thermo Scientific, Rockford, IL). All elution fractions of the C2 domain were removed from the fridge (4 °C) and each of the samples were prepared with 20 µL of protein and 5 µL of 5X Gel Loading Dye. The protein samples were run on a 15% polyacrylamide gel using the Mini Protean III system from BioRad. The gel was run at room temperature with a voltage of 70V for stacking and 120V for separating gel with freshly prepared 1X SDS running buffer (25 mM Tris-base, 192 mM glycine, and 0.1% SDS). The protein bands were visualized by first staining with Fairbank A (25% isopropanol, 10% acetic acid, 0.05% Coomassie), heated in the microwave for 20s, and then rocked for 10 min. The gel was then stained in the same procedure with Fairbank B (10% Isopropanol, 10% Acetic Acid, 0.005% Coomassie) and Fairbank

C (10% Acetic Acid, 0.002% Comassie). Fairbank D (10% acetic acid) was added, heated in the microwave for 20s, and then rocked to de-stain the gel. A kim wipe was placed after 10min to absorb the stain. Milli Q water was added to prevent the gel from dehydrating and the gel was rocked overnight. The elution fractions with the highest purity and yield of protein were pooled together and concentrated to 1.5 mL using 3,000 MWCO Centricon tubes (Fisher Scientific, Chicago, IL).

Bicinchoninic Acid Assay

The protein concentration was determined using bicinchoninic acid (BCA) assay. The protein samples were diluted as follows: 2 µL of protein with 13 µL buffer and 1 µL protein with 14 µL of buffer (20mM HEPES, 300mM NaCl, pH 7.4). For the BCA assay, 15µL of the diluted protein sample and 120µL of 1 part of Copper (II) Sulfate Solution (Thermo Scientific, Rockford, IL) and 49 part of BCA buffer (Thermo Scientific, Rockford, IL) were added to a 96-well u-bottom micro-titer plate. The samples were mixed thoroughly and incubated for 60 min at 37°C. After 60 min, the micro-titer plate was read at 595nm on a Perkin Elmer Victor^3 Multilabel Reader using Wallace 1420 Manager software. The concentration was determined from the standard curve with known BSA concentrations using the mean and standard deviation of the triplicate set.

After determining the protein concentration, aliquots of 125µg protein sample were lyophilized overnight and stored at -20˚C.

FTIR-ATR Spectroscopy

To prepare the protein samples for the FTIR-ATR analysis, 125μg of lyophilized protein was dissolved in 15μL D_2O buffer, containing 10mM HEPES, 160mM KCl, 10mM CaCl2, pH 6.5. The POPC and PI(4,5)P_2 lipids (Avanti, Alabaster, AL) were stored in chloroform at 0.28 μg/μL at -20°C. Lipid films were prepared by drying the appropriate amount of the lipid stock solution in a stream of nitrogen at room temperature. The samples were dried overnight in vacuum at 45-50°C to completely remove the organic solvent. Mixed multilamellar lipid vesicle/protein samples were obtained by re-suspending the appropriate lipid mixtures with 125μg protein solution. The protein-bearing samples included 1 mole protein per 8 moles of POPC. After adding the protein solution to the dried lipid samples, the samples were vortexed three times for 60s at in intervals of 5 min.

FTIR-ATR experiments were carried out with a Bruker Tensor 27 spectrometer (Bruker, Munich, Germany) with a LN-MCT (Internal) detector. The spectrometer was cooled with liquid nitrogen for 1h before use. Interferograms were collected at 2 cm^{-1} resolution (512 scans) at 40Hz scan speed, apodized with a Blackman-Harris 3-Term function, and Fourier transformed with two level of zero filling to yield spectra encoded between 4000 cm^{-1} to 750 cm^{-1}. Using a Q-tip, the ATR plate was cleaned with hexane, isopropanol (or Chloroform/Methanol 2:1) and D_2O. The cap was screwed on quickly to avoid contact with H_2O in the air. The background single channel was recorded (512 scans). 15 μL of protein sample was added onto the ATR cell. The sample single channel was checked (16 scans) to see if the water noise is small, and then recorded for three times (512 scans). Spectra of the mixture of protein and lipid were measured to determine

the secondary structure. Background scans were recorded for every round of sample scans.

After the completion of protein/lipid FTIR-ATR experiments, buffer spectra (with quick contact with air) were obtained to match the water peak in the spectra of the protein samples. The water vapor spectrum was subtracted from the protein spectra and the buffer spectra, respectively, and then the matched buffer was subtracted from the protein spectrum using OPUS software. The reported spectra were smoothed with a factor of 13.

Results and Discussion

Optimization of cPLA$_2$α C2 domain Expression and Purification

The same amount of LB broth, kanamycin 30µg/mL, and the C2 domain glycerol stock were incubated for 2.5 hr when the OD_{600nm} reached 0.675. Then the cell was induced with different concentrations of IPTG (50µM and 100µM and incubated at different temperatures (18°C and 37°C). The optical density was measured after induction for 1 hr, 2 hr, 3hr, 4hr, 6hr and overnight to compare which condition produced the greatest amount of soluble protein. When the cells were induced with 50µM IPTG and grew under 18°C overnight, largest amount of cell pellet was harvested (Table 1).

	Flask 1	Flask 2	Flask 3	Flask 4
LB broth (mL)	25 mL	25 mL	25 mL	25 mL
Kanamycin 30mg/mL (µL)	25 µL	25 µL	25 µL	25 µL
C2 domain stock added (mL)	0.273 mL	0.273 mL	0.273 mL	0.273 mL
Optical Density (OD) after 2.5 hr	0.675	0.675	0.675	0.675
IPTG conc. (µM)	50 µM	100 µM	50 µM	100 µM
Incubation Temperature (ºC)	37 ºC	37 ºC	18 ºC	18 ºC
OD after 1 hr	1.618	1.854	X	X
OD after 2 hr	2.46	2.73	1.502	1.278
OD after 3 hr	2.57	3.67	X	X
OD after 4 hr	X	X	3.08	2.29
OD after 6 hr	X	X	5.57	4.67
OD overnight	X	X	16.36	12.52

Table 1. Optical Density Table of the Optimization of Cell Growth

The protein was purified from both, the soluble fraction, where the protein is folded in its original secondary structure, and the insoluble fraction (inclusion bodies). A faint 15kDa band was observed in the soluble fraction and a much stronger band was observed in the insoluble fraction (Figure 8), which means most of the protein were in the insoluble fractions. Therefore, the protein was purified from the inclusion bodies in the cell pellet. The inclusion bodies were solubilized in 2mL of 8M Urea Buffer and dialyzed against decreasing concentrations of urea buffer (8M→6M→4M→2M→0M) for a total of three days. A large amount of the protein precipitated out during dialysis. The SDS-PAGE of the protein after dialysis indicated a low protein yield (Figure 9). This suggested that dialysis for a long time triggered protein aggregation and caused the protein to precipitate. Therefore, to avoid aggregation and precipitation, the protein needed to be refolded in a shorter amount of time.

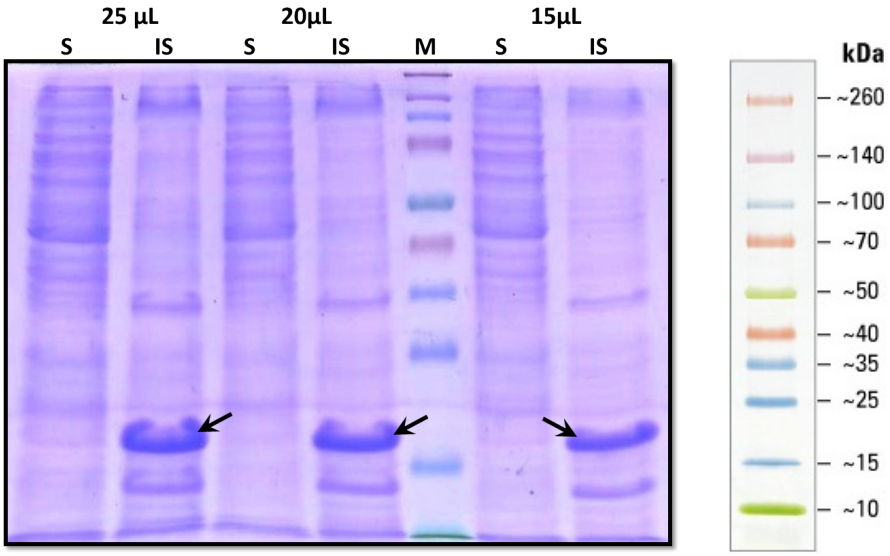

Figure 8. SDS-PAGE of cPLA$_2$α C2 domain in supernatant and pellet after cell lysis and before purification. S – soluble fraction (supernatent), IS – insoluble fraction (pellet), M – protein ladder. Arrow indicating the C2 domain protein

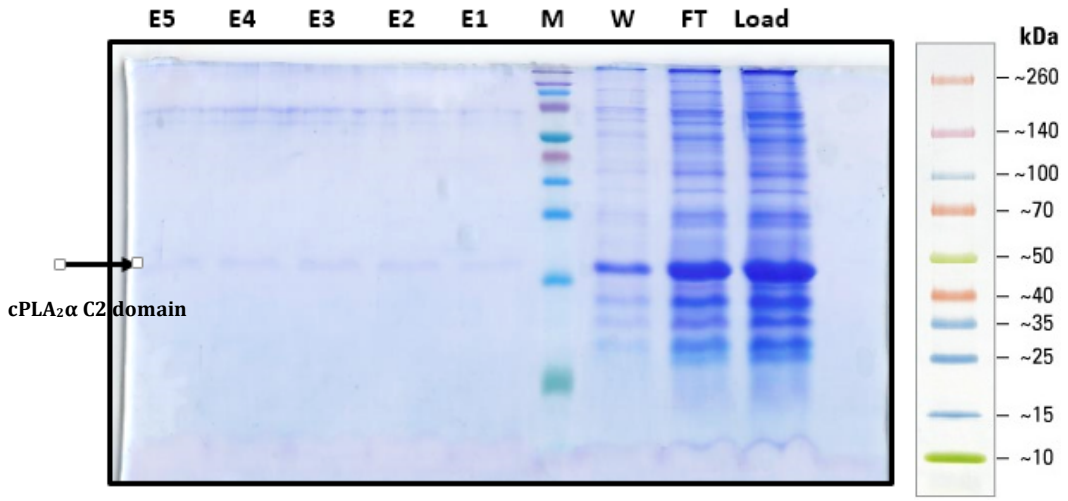

Figure 9. SDS-PAGE of the C2 domain after dialysis. E1-E5 – elution fraction 1 to 5, M – protein ladder, W – wash, FT – flow through

Purification of cPLA$_2$α C2 Domain under Denaturing Conditions

To shorten the overall refolding process, the protein was refolded and purified on a Ni-NTA agarose column. After the cell pellet was solubilized with 8M urea buffer, the solution was passed through the Ni-NTA column. The denatured protein was washed with phosphate buffer at pH 6.3 and then refolded on the column using a urea gradient buffer utilizing fast protein liquid chromatography (FPLC). The refolding process took around 2 hrs and the DLS measurements after Ni-NTA columns suggested the protein was monomeric (diameter in volume PSD was ~ 3.1 nm). Unfortunately, the process was not reproducible as the denatured 6His-tagged protein showed a low binding affinity to Ni-NTA column, which led to a low yield; however, the protein was greater than 90% pure (Figure 10). The major problem encountered in this method is the low binding affinity of the denatured protein to the Ni-NTA column. In order to increase the binding

affinity and to achieve a higher yield, we tried to refold first the protein and to purify the folded protein with the Ni-NTA column.

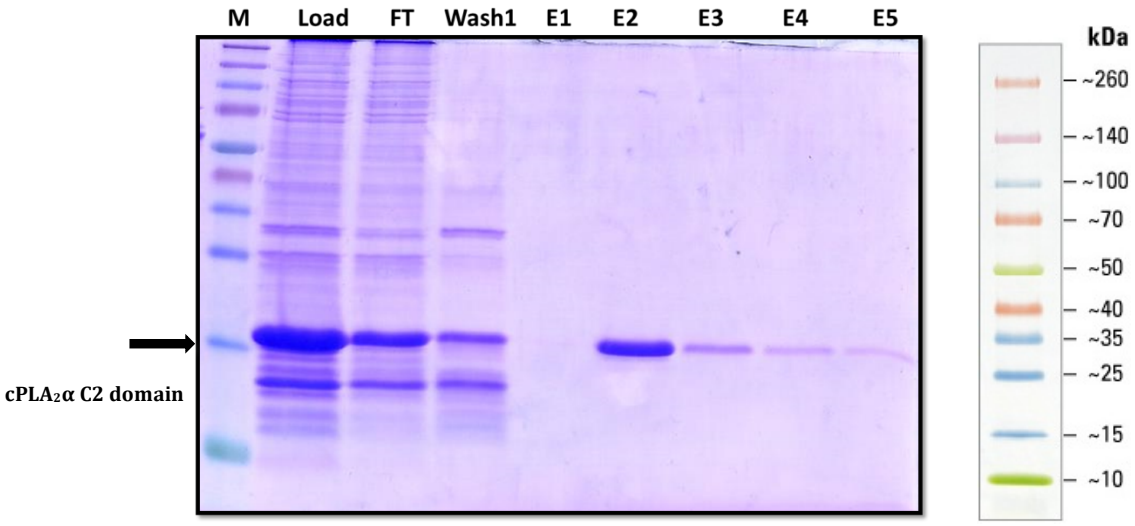

Figure 10. SDS-PAGE of the C2 domain refolded on column. M – protein ladder, FT – flow through, E1-E5 – elution fraction 1 to 5

Purification of cPLA$_2$α C2 Domain under Native Conditions

To obtain a properly folded cPLA$_2$α C2 domain, the protein was first dialyzed against urea buffer with decreasing concentration (8M→1.5M→0M). Different from the initial dialysis, the overall volume of the solubilized cell pellet in 8M Urea was increased from 2mL to 30mL and the protein was dialyzed for no more than a 24hr period. Next, the protein was purified on a Ni-NTA column with different concentrations of imidazole (washed with 10mM and 20mM, and eluted with 300M) (Figure 11 and 12). Although the purity of the C2 domain obtained under native condition was not as high as the purity obtained under dantured condition, a higher yield of protein was obtained and this protein preparation was used for the FTIR-ATR experiments.

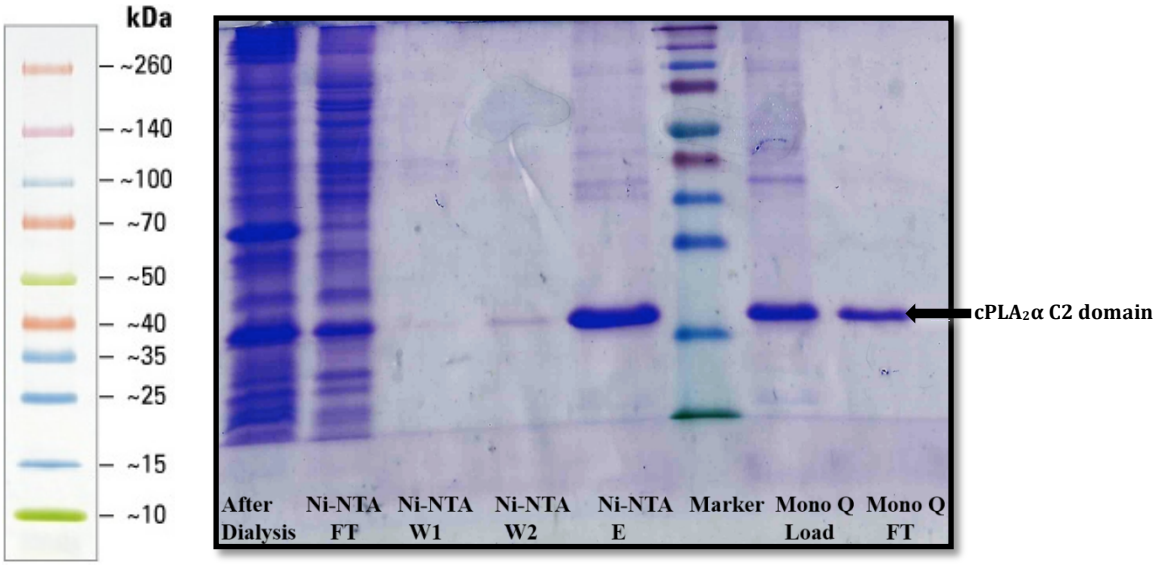

Figure 11. SDS-PAGE of the C2 domain purified with Ni-NTA column after dialysis. FT – flowthrough, W – wash, E – elution

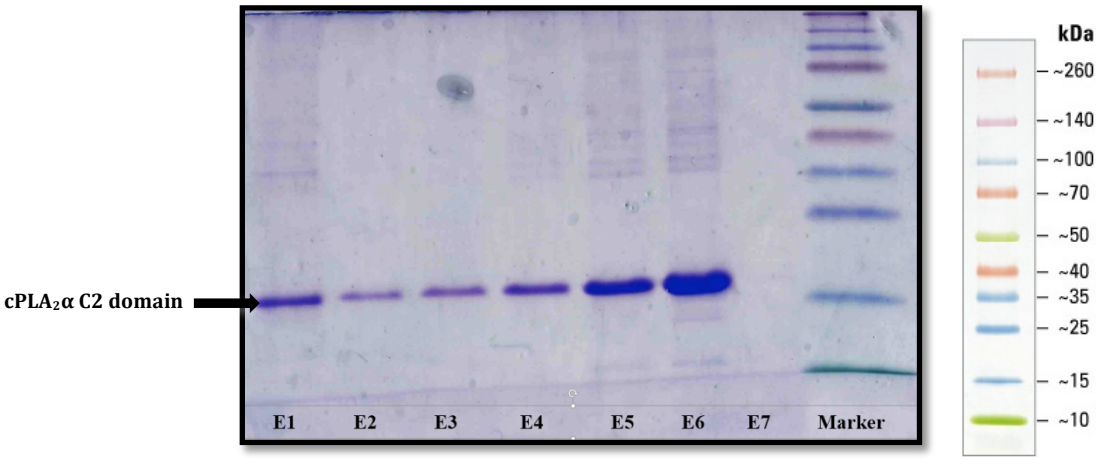

Figure 12. SDS-PAGE of 7 elution fractions after purification with Mono Q column. E1-E7 – elution fraction 1-7

Estimation of cPLA$_2$α C2 Protein Concentration with BCA Assay

The elution fractions with the highest purity and yield of protein were pooled and concentrated, and then the BCA assay was used to determine the concentration of protein.

The protein concentration was estimated from the BSA standard curve (Figure 13). On average, a protein concentration of 1.15mg/mL was obtained (Table 2).

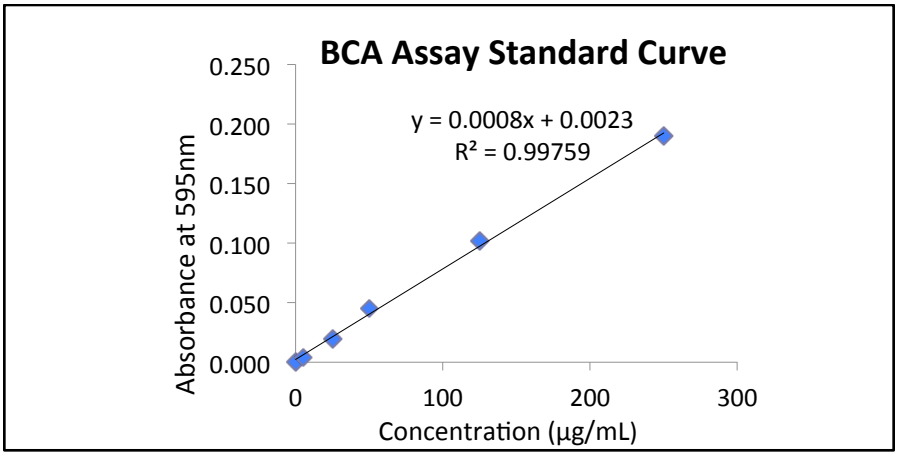

Figure 13. BCA Assay standard curve

	Sample Volume (µL)	Avg A595	Blanked	Dilution Conc.(µg/mL)	Calculated Conc.(µg/mL)	Avg Conc. (µg/mL)
C2 Domain Concentrated	2	0.188	0.112	136.531	1023.984	1152.537
	1	0.147	0.071	85.406	1281.091	

Table 2. Calculations of the protein concentration

Secondary Structure Changes of cPLA2α C2 Domain upon lipid binding

FTIR-ATR measurements require a high concentration of the protein of interest (125µg/15µL). Purification using lyophilization was used rather than purification using dialysis to obtain the amount of protein required for the FTIR-ATR experiments. When preparing the protein sample, the lyophilized protein did not completely dissolve in the D_2O buffer. A cloudy solution was observed with a lot of air bubbles. Bath sonication of the sample at room temperature and adjusting the pH of the buffer (pH 7.4 and pH 6.5)

were tried to increase the solubility of the protein. A cloudy solution was still observed with both methods. Two samples were combined together to increase the volume and the protein sample was carefully pipetted. To avoid aggregation, the protein sample was kept on ice at all times. The protein sample was measured by DLS before applying it to the ATR cell and a diameter of over 100nm was obtained. This partial protein aggregation could not be avopided as the protein does not fully dissolve in the D_2O buffer.

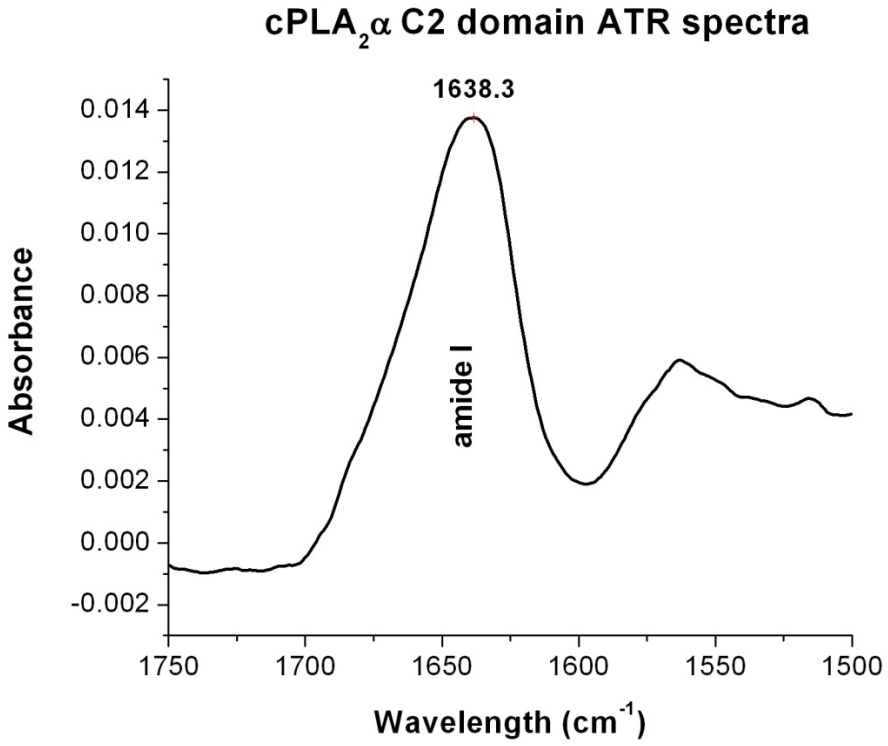

Figure 14. IR-ATR spectra of the C2 domain alone

An FTIR-ATR spectrum of the $cPLA_2\alpha$ C2 domain in the absence of lipids was obtained (Figure 13). The peak at 1638 cm^{-1} indicated that the protein has predominantly a β-sheet secondary structure and that the protein was not aggregated (otherwise a band at ~1619 cm^{-1} would have been obtained). This result indicated that the aggregation of the protein was less pronounced than it was inferred from the DLS measurements. Because

the protein was not completely dissolved in the D_2O buffer, the exact amount of the protein in the solution was unknown. Therefore, the experiment cannot be repeated with exactly the same protein concentration, and the spectra of the C2 domain obtained in two repeat experiments showed the same position of the amide I band, indicating a predominant β sheet secondary structure, but the amide bands for the two experiments showed different intensities.

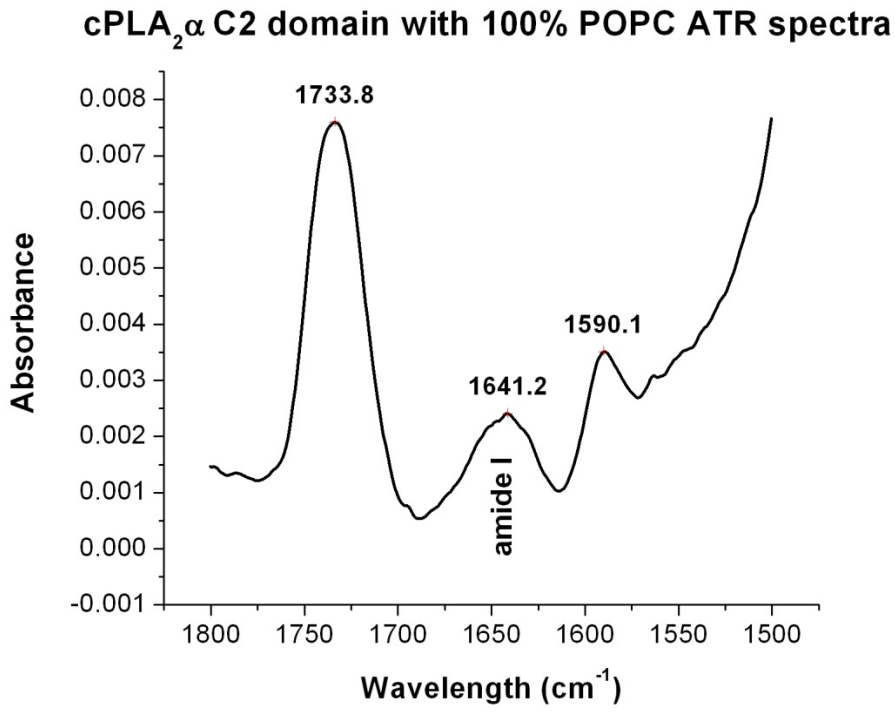

Figure 15. FTIR-ATR spectra of the C2 domain bound to POPC vesicles

After obtaining an FTIR-ATR spectrum of the C2 domain alone, an FTIR-ATR spectrum of the $cPLA_2\alpha$ C2 Domain in the presence of POPC vesicles was obtained to compare how POPC affects the secondary structure of the C2 domain (Figure 14). The band at 1733 cm^{-1} is associated with the C=O stretching vibration of the lipid carbonyl groups, while the peak at 1641 cm^{-1} in the amide I region indicates that the protein has predominantly a β sheet secondary structure and that the protein was not aggregated. The

slight shift of the band relative to the lipid free spectrum is presumably an artifact to the fact that the band is quite weak, resulting in difficulties when the buffer spectrum is subtracted out. The peak at 1590 cm^{-1} might be associated with the amide II vibration, however, the position is somewhat unusual and for a completely D_2O exchanged protein, this band should be absent in the spectrum.. Compared to the spectrum of the C2 domain alone, the amide I band indicating β sheet shift to the left for 3 cm^{-1}, mainly remained unchanged, but with a lower intensity. The lower intensity is probably due to only weak binding of the protein to the lipids. Since the lipid vesicles settle on the ATR crystal, they displace the protein from the crystal, resulting in a lower intensity. However, the effect of POPC on the C2 domain secondary structure was found to be minor.

The protein spectrum in the presence of POPC needs further investigation. The amide I band intensity is poor and therefore, it is difficult to draw conclusive results from these measurements.

Future Work

The first step of moving forward would be to reproduce the spectra of the C2 domain when bound to POPC vesicles. The reproduced results should confirm that PC does not affect the major secondary structure of the C2 domain.

The ultimate goal of this project was to understand the binding properties and change of orientation of the cPLA$_2$α C2 domain in the presence of C1P. To achieve this goal, FTIR-ATR experiments of the C2 domain bound to 97% PC 3% C1P will be carried out, and then the spectra will be compared to the spectrum of the C2 domain alone. The difference between the two spectra, especially the peaks in the amide I spectral region, would indicate whether the C2 domain remained in a predominantly β sheet structure. Since the C1P binding site in cPLA$_2$ C2 domain is on the β groove, a secondary change or a change of protein orientation is expected.

Other lipid compositions, such as 97% PC, 3%PI(4,5)P$_2$ will be used to compare the interaction between the C2 domain and PI(4,5)P$_2$ and C1P, respectively. This comparison is expected to increase our understanding about the specificity of the C2 domain/C1P binding.

References

[1] Clark, J. D.; Schievella, A. R.; Nalefski, E.A.; Lin, L, L. *J. Lipid. Mediat.* **1995**, 12, 83.

[2] Dessen, A.; Tang, J.; Schimidt, H.; Stahl, M.; Clark, J.D.; Seehra, J. Somers, W.S. *Cell.* **1999**, 97, 349.

[3] Leslie, C.C.*J. Biol.Chem*. **1997**, 272, 16709.

[4] Stahelin, R. V.; Subramanian, P.; Vora, M.; Cho, W.; Chalfant, C. E. *J. Biol. Chem.* **2007**, 282, 20467.

[5] Evans, J. H.; Spencer, D. M.; Zweifach, A.; Leslie, C. C. *J. Biol. Chem.* **2001**, 276, 30150.

[6] Kerkelä, R.; Boucher, M.; Zaka, R.; Gao, E.; Harris, D.; Piuhola, J.; Song, J.; Serpi, R.; Woulfe, K. C.; Cheung, J. Y. *Clin. Transl. Sci.* **2011**, 4, 236.

[7] Hewson, C. A.; Patel, S.; Calzetta, L.; Campwala, H.; Havard, S.; Luscombe, E.; Clarke, P. A; Peachell, P. T.; Matera, M. G.; Cazzola, M. *J. Pharmacol. Exp. Ther.*
2012, 340, 656.

[8] Tai, N.; Kuwabara K.; Kobayashi, M.; Yamada, K.; Ono, T.; Seno, K.; Gahara, Y.; Ishizaki, J.; Hori, Y. *Inflamm. Res.* **2010**, 59, 53.

[9] Sundarraj, S.; Kannan, S.; Thangam, R.; Gunasekaran, P. *J. Cancer Res. Clin. Oncol.* **2012,** 138, 827.

[10] Gentile, M. T.; Recci, M. G.; Sorrentino, P. P.; Vitale, E.; Sorrentino, G.; Puca, A. A.; Colucci-D'Amato, L. *Mol. Neurobiol*. **2012,** 45, 596.

[11] Subramanian, P.; Stahelin, R.V.; Szulc, Z.; Bielawska, A.; Cho, W.; Chalfant, C. E. *J. Biol. Chem.* **2005,** 280, 17601.

[12] Frazier, A. A.; Wisner, M. A.; Malmberg, N. J.; Victor, K. G.; Fanucci, G. E.; Nalefski, E. A.; Falke, J. J.; Cafi, D. S. *Biochemistry.* **2002,** 41, 6282.

[13] Málková, S.; Long, F.; Stahelin, R. V.; Pingali, S. V.; Murray, D.; Cho, W.; Schlossman, M. L. *Biophys. J.* **2005,** 89, 1861.

[14] Casas, J.; Gijon, M. A.; Vigo, A. G.; Crespo, M. S.; Balsinde, J.; Balboa, M. A. *Mol. Biol. Cell.* **2006,** 17, 155.

[15] Wijesinghe, D.S.; Subramanian, P.; Lamour, N. F.; Gentile, L. B.; Granado, M. H.; Bielawska, A.; Szulc, Z.; Gomez-Munoz, A; Chalfant, C. E. *J. Lipid Res.* **2009,** 50, 1986.

[16] Ward, K. E.; Bhardwaj, N.; Vora, M.; Chalfant, C. E.; Lu, H.; Stahelin, R. V. *J. Lipid Res.* **2013**, 54, 636.

[17] Subramanian, P.; Vora, M.; Gentile, L. B.; Stahelin, R. V.; Chalfant, C. E. *J. Lipid Res.* **2007,** 48, 2701.

[18] Kooijman, E. E.; Vaknin, D.; Bu, W.; Joshi, L.; Kang, S.W.; Gericke, A.; Mann, E. K.; Kumar, S. *Biophys. J.* **2009**, 96, 2204.

[19] Punnia-Moorthy, A. *J. Oral Pathol.* **1987,** 16, 36.

[20] Gerweck, L. E.; Seetharaman, K. *Cancer Res.* **1996**, 56, 1194.

Appendix A Chemical Information

Chemical	Manufacturer
Calcium Chloride anhydrous	Fisher Scientific (Fair Lawn, NJ, USA)
Chloroform	Fisher Scientific (Fair Lawn, NJ, USA)
D_2O	Cambridge Isotope Laboratories (Andover, MA, USA)
Deoxycholate sodium salt	Amresco (Solon, OH, USA)
EDTA disodium salt	Amresco (Solon, OH, USA)
Glycerol	Amresco (Solon, OH, USA)
HEPES	Fisher Scientific (Fair Lawn, NJ, USA)
Imidazole	Alfa Aesar (Ward Hill, MA, USA)
Isopropyl-1-thio-β-D-galactopyranoside (IPTG)	Alfa Aesar (Ward Hill, MA, USA)
Kanamycin sulfate	Amresco (Solon, OH, USA)
Phenylmethylsulfonyl fluoride (PMSF)	Amresco (Solon, OH, USA)
Potassium Chloride	Fisher Scientific (Fair Lawn, NJ, USA)
Sodium Chloride	VWR (West Chester, PA, USA)
Tris-Hydrochloride	Fisher Scientific (Fair Lawn, NJ, USA)
Triton-X-100	Sigma (St. Louis, MO, USA)
Bacto Tryptone	BD (Sparks, MD, USA)
Urea	G-Bioscience (St. Louis, MO, USA)
Yeast Extract Powder	Affymetrix (Cleveland, OH, USA)

Appendix B Acronyms

$C_{18:1}$-C1P: D-erythro-Ceramide C18 1 Phosphate

EDTA: ethylenediaminetetraacetic acid

IPTG: isopropyl-1-thio-β-D-galactopyranoside

PI(4,5)P_2: phosphatidylinositol 4,5-bisphosphate

PMSF: phenylmethylsulfonyl fluoride

POPC: 1-palmitoyl-2-oleoyl-sn-glycero-3-phosphocholine

Appendix C Buffer Composition

LB broth
10g Tryptone
5g yeast extract
10g NaCl

2X YT broth:
16g Tryptone
10g yeast extract
5g NaCl
4mL 100% Glycerol

Lysis buffer:
50mM Tris-HCl **pH 8.0**
50mM NaCl
2mM EDTA
1mM PMSF
0.4% (v/v) Triton-X-100
0.4% (w/v) sodium deoxycholate

Wash Buffer 1:
50mM Tris-HCl **pH 8.0**
50mM NaCl
2mM EDTA
0.8% (v/v) Triton-X-100
0.8% (w/v)sodium deoxycholate

Wash Buffer 2:
50mM Tris-HCl **pH 8.0**
5M Urea
5mM EDTA

Solubilizing Buffer:
50mM Tris-HCl **pH 8.0**
8M Urea
5mM EDTA

Dialysis Buffer 1:
50mM Tris-HCl **pH 8.0**
1.5M Urea

Dialysis Buffer 2:
50mM Tris-HCl **pH 8.0**

Binding Buffer:
50mM Tris-HCl **pH 8.0**
150mM NaCl
10mM imidazole

Wash Buffer 3:
50mM Tris-HCl **pH 8.0**
150mM NaCl
20mM imidazole

Elution Buffer 1:
20mM HEPES **pH 8.0**
150mM NaCl
400mM imidazole

Dialysis Buffer 3:
20mM HEPES **pH 7.4**
100mM NaCl

Low Salt Buffer:
20mM HEPES **pH 7.4**
50mM NaCl

High Salt Buffer:
20mM HEPES **pH 7.4**
1M NaCl

Elution Buffer 2:
20mM HEPES **pH 7.4**
300mM NaCl

D_2O Buffer:
20mM HEPES **pH 7.4**
160mM KCl
10mM $CaCl_2$

Appendix D Instruments

Beckman Coulter Avanti J Series Centrifuges and JA-25.5 Rotor (Beckman Coulter, Danvers, MA)

Bruker Tensor 27 (Brukeroptics, Billerica, USA)

Innova 4335 Refrigerated Incubator Shaker (New Brunswick Scientific, Enfield, CT)

Perkin Elmer Victor^3 Multilabel Reader (Perkin Elmer, Waltham, MA)

Sonic Dismembrator Model 100 (Fisher Scientific, Fair Lawn, NJ)

Zetasizer Nano ZS (Malvern, Worcestershire, UK)